

Article

Not peer-reviewed version

---

# Seismicity of the Noto Peninsula: Spatial Patterns, Shallow Seismic Zones, and Potential Volcano-Related Signals

---

[Tomokazu Konishi](#) \*

Posted Date: 2 March 2026

doi: 10.20944/preprints202601.2352.v2

Keywords: earthquake prediction; seismic visualization; magnitude locator; scale; shallow seismicity



Preprints.org is a free multidisciplinary platform providing preprint service that is dedicated to making early versions of research outputs permanently available and citable. Preprints posted at Preprints.org appear in Web of Science, Crossref, Google Scholar, Scilit, Europe PMC.

Copyright: This open access article is published under a [Creative Commons CC BY 4.0 license](#), which permit the free download, distribution, and reuse, provided that the author and preprint are cited in any reuse.

Article

# Seismicity of the Noto Peninsula: Spatial Patterns, Shallow Seismic Zones, and Potential Volcano-Related Signals

Tomokazu Konishi

Graduate School of Bioresource Sciences, Akita Prefectural University, Akita 010-0195, Japan; konishi@akita-pu.ac.jp

## Abstract

The Noto Peninsula is a seismically active region where spatial patterns and shallow seismic zones play a critical role in understanding earthquake behavior. While visualization techniques for seismicity have advanced, their effective application still requires practical experience and region-specific interpretation, as earthquake susceptibility varies spatially. In this study, we analyze earthquake catalogues and mesh-based magnitude parameters for events occurring between 2023 and 2024 to investigate seismic anomalies in the region. Temporal variations in the magnitude locator and scale, combined with spatial patterns of shallow seismicity, reveal anomalous behavior in the offshore area west of Noto. This area is characterized by persistently elevated locator values and locally reduced scale—features that resemble precursory patterns observed in volcanic settings. The seismic sequences of 5 May 2023 (M6.5) and 1 January 2024 (M7.6) illustrate how such combined signals may precede large events, while also highlighting how aftershock decay and resurgence complicate post-event energy assessments. These findings suggest the possible influence of submarine volcanic or volcano-related structures, as well as ongoing orogenic deformation. The results support the need for continued, targeted monitoring of epicentral activity in this region and may offer insights applicable to other tectonically complex areas.

**Keywords:** earthquake prediction; seismic visualization; magnitude locator; scale; shallow seismicity

---

## 1. Introduction

Japan is located at the convergence of multiple tectonic plates, making it one of the most seismically active regions in the world [1]. Given the sudden and often devastating nature of earthquakes, the development of reliable prediction methods has long been a critical goal. Despite decades of research, however, earthquake prediction has remained elusive [2].

Recent studies, including a new review [3], suggest that prediction may be feasible through the application of exploratory data analysis (EDA) to simple seismic measurements. EDA has revealed, for example, that earthquake magnitudes follow a normal distribution—an observation that challenges the long-standing Gutenberg–Richter (GR) law (see Appendix A). Similarly, traditional models describing aftershock decay, such as the Omori rule, have been re-evaluated and significantly revised. These findings raise fundamental questions about how seismic energy should be characterized and assessed. As a result, our theoretical understanding of earthquake processes may be on the cusp of substantial transformation.

However, significant challenges remain. Using the mesh-based visualization method together with three-dimensional inspection of seismicity [3] provides two complementary perspectives for monitoring earthquake activity. These approaches have enabled the identification of precursory patterns associated with earthquakes above a certain magnitude [3]. Nevertheless, practical experience is often required to interpret these signals reliably. A key challenge is the strong regional variability in seismic behavior. I have not proposed a universal criterion for anomaly detection

because such a standard is unlikely to be valid across Japan's diverse tectonic environments. If all regions shared identical geological structures, a single threshold might be feasible. In reality, however, some areas are inherently more prone to large earthquakes than others, making uniform criteria inappropriate.

One such region is the Noto Peninsula. Although located far from major plate boundaries, Noto lies above a complex interaction zone involving the Eurasian Plate, the Pacific Plate, and the Philippine Sea Plate. In particular, the shallow seismic zone associated with the Sanriku–Oki segment of the Pacific Plate's subduction extends beneath this region. This zone is interpreted as an area where compressive stress accumulates as the Pacific Plate pushes horizontally against the overriding Eurasian Plate. Such stress transfer is thought to generate a near-surface environment favorable for frequent shallow earthquakes [3]. Although the main plate boundary lies at depth, the mechanical coupling between the subducting and overriding plates may transmit stress upward into the crust, creating a persistent seismogenic zone beneath Noto.

In 2023, this region exhibited a marked increase in the magnitude locator, accompanied by a rise in event scale (Figure 1A–B). Because earthquake magnitudes follow an approximately normal distribution [3], it is straightforward to track temporal variations in its two parameters: the mean ( $\mu$ ), represented by the locator, and the standard deviation ( $\sigma$ ), represented by the scale. An increase in both parameters is typically associated with heightened potential for large earthquakes [3]. Indeed, a magnitude 6.5 earthquake struck the area on 5 May 2023.

In this study, we examine seismic activity using a latitude–longitude grid of 1°. Based on empirical experience, this resolution offers a practical balance for analyzing earthquakes in Japan: smaller grids tend to yield insufficient data for statistical analysis, while larger grids reduce the spatial precision of event localization [5]. I revisit this choice in a later section. During the period from October to December 2023—after the aftershock sequence had largely decayed—the locator remained elevated, although the scale had decreased (Figure 1C–D). Shortly thereafter, on 1 January 2024, a magnitude 7.6 earthquake occurred. If the persistently high locator had been disregarded, this event would have appeared unpredictable. How should this pattern be interpreted? The following sections examine this question in detail.

The purpose of this study is to identify seismic anomalies in the Noto Peninsula—an area of frequent seismic activity—and to explore how such anomalies might be used for earthquake prediction. This region is home to many communities that have long lived under the threat of seismic disasters and have an urgent need for effective forecasting methods. The analysis centers on the January 2024 earthquake, which damaged approximately 165,000 homes. As of January 2026, two years later, 90% of those affected remain in temporary housing, with few having returned to normal life. The human toll was also severe. While prediction cannot eliminate disasters, it can help mitigate their consequences. As with weather forecasting, seismic prediction must rely on the best available data, even if imperfect. It is both reasonable and necessary to act on what is known. It is my hope that the insights gained here will contribute to improving preparedness in other earthquake-prone regions as well.

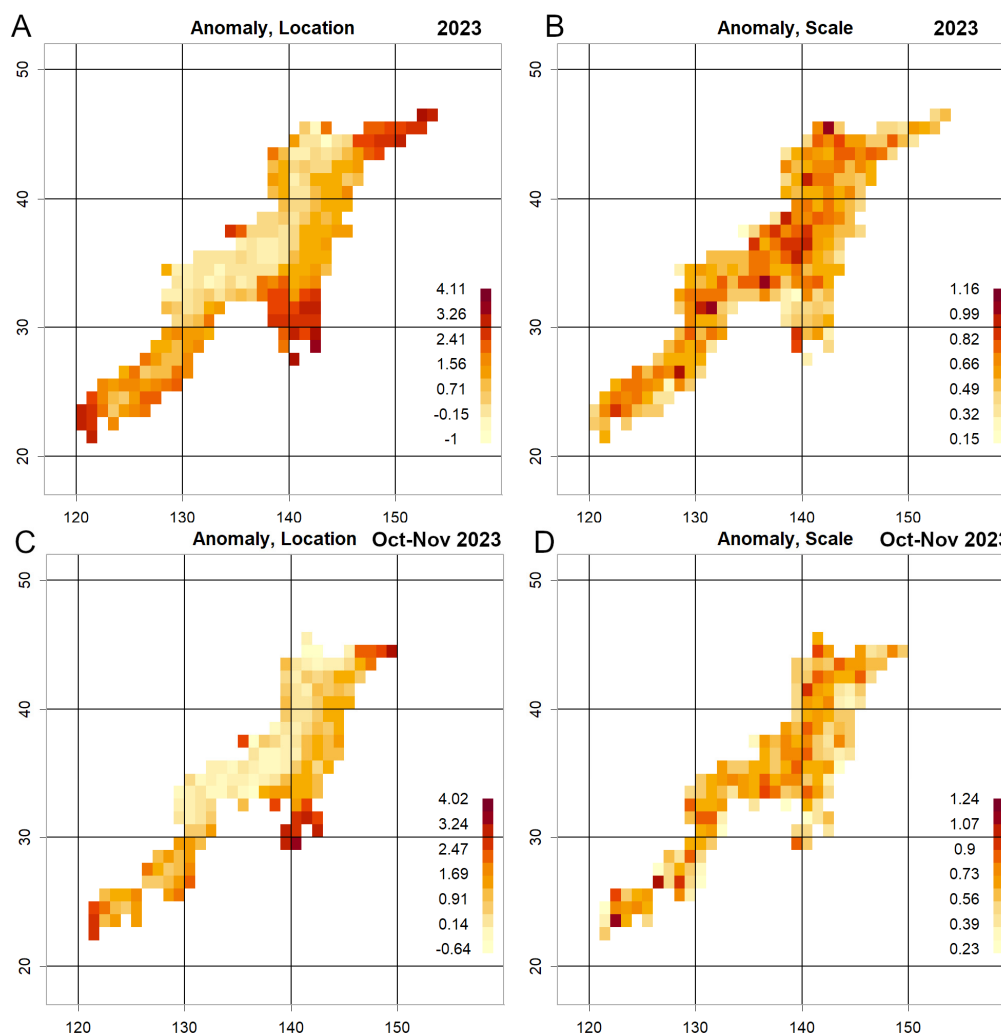


**Figure 1. A–B.** Magnitude-based anomaly metrics for all earthquakes in 2023 [1]. **A.** Locator. **B.** Scale. Both parameters show elevated values around the Noto Peninsula (approx. 37°N, 137°E). **C–D.** Data from October 2023 onward, after aftershocks from the May 2023 earthquake had largely subsided. **C.** Locator. **D.** Scale. The locator remains elevated, whereas the scale appears to have returned to normal levels. The Noto Peninsula is located approximately between 136.7°E–137.3°E and 36.8°N–37.5°N. In Figure 1A, elevated locator values appear in the two adjacent panels spanning 134°–136°E and 37°–38°N. In Figure 1C, the panel at 135°–136°E also shows elevated values. These regions correspond to the shallow offshore area northwest of the Noto Peninsula. In contrast, Figure 1B shows elevated scale values across a broader area. The primary region of interest in this panel is the tip of the Noto Peninsula, located at 137°–138°E and 37°–38°N.

## 2. Material and Methods

The analysis followed an exploratory data analysis framework, which is well suited for identifying structural patterns in scientific datasets. Earthquake data were obtained from the catalogues published by the Japan Meteorological Agency (JMA) with the most recent entries downloaded daily from the same source.

Figure 7A in Appendix A utilizes monthly summary data [8], which includes only perceptible earthquakes [8]. As this figure exhibits a strong linear relationship, the summary data can be considered fundamentally complete—reliable even for magnitudes as low as  $M = 1$ . In contrast, the full catalogue includes events down to approximately  $M = -1$ , representing one-thousandth the energy of  $M = 1$  events. At these lower magnitudes, data gaps are inevitable.

When plotting a normal Q–Q plot using the full catalogue, the lower data points deviate downward, resulting in a concave curve. This distortion is likely due to detection limitations in offshore regions, where seismometers are sparse. Nevertheless, the Latitude–Longitude Mesh

Analysis (Figure 1) sufficiently covers land areas, and this limitation does not significantly affect the predictive analysis conducted here. Moreover, the analytical method was designed to accommodate such data characteristics [3].

All computations were performed using the R statistical environment [7], and the full R code used in this study is available via Zenodo [3]. This study does not engage extensively with long-standing theoretical discussions on the nature of earthquakes. There are several reasons for this. First, many of these discussions rely on assumptions that are difficult to test or falsify in a scientific sense [9], which limits their utility for empirical validation. For example, clustering analyses often require numerous unverifiable premises. Similarly, while research on volcanic formation has produced many insightful hypotheses, these have yet to be substantiated through direct observation or predictive success. Moreover, it remains unclear whether the present study areas correspond to regions where such theories are applicable.

A more fundamental reason is that many of these frameworks are grounded in the Gutenberg–Richter law and the Omori rule—models that, while historically influential, have undergone significant revision in recent years [3]. As both pertain to seismic energy distributions, theoretical systems based on them may require substantial re-evaluation [2]. The present study adopts a different analytical framework, and as such, prior models built on these assumptions were not referenced.

### 3. Results and Discussion

Figure 2A shows a linear decrease on a semi-logarithmic plot following the earthquake on 5 May 2023. Two distinct segments are evident, indicating different decay rates with distinct half-lives—a pattern commonly observed in aftershock sequences from many other earthquakes [3]. The observed decay rate differs markedly from that predicted by Omori's formula [10], which assumes an inverse power-law dependence, and from its modified form, known as the Omori–Utsu formula [11]. The initial assumption of inverse proportionality was therefore inappropriate [3].

Similarly, in typical large events, the magnitude locator increases by approximately 2–4 units and then decays rapidly with a short half-life [3]. In the present case, this pattern was scarcely observed. The figure displays hourly averages; when the window is extended to 12 hours, the transient increase nearly disappears. Instead, the locator rose again around September–October, exceeding the level observed on 5 May (corresponding to the anomaly in Figure 1C). This behaviour is unusual.

Both earthquake frequency and earthquake energy follow log-normal distributions [3], implying that they are governed by the multiplicative interaction of several underlying factors. However, the half-lives associated with these two quantities differ. Consequently, the final factor that triggers an earthquake differs between the phenomenon governing whether an earthquake occurs and the phenomenon governing its magnitude. For the 5 May event, the factors regulating earthquake occurrence appear to have been sufficiently aligned, whereas the factors contributing to larger magnitude growth were not. This suggests that the seismic energy released during the 5 May earthquake may have been insufficient to fully relax the accumulated stress.

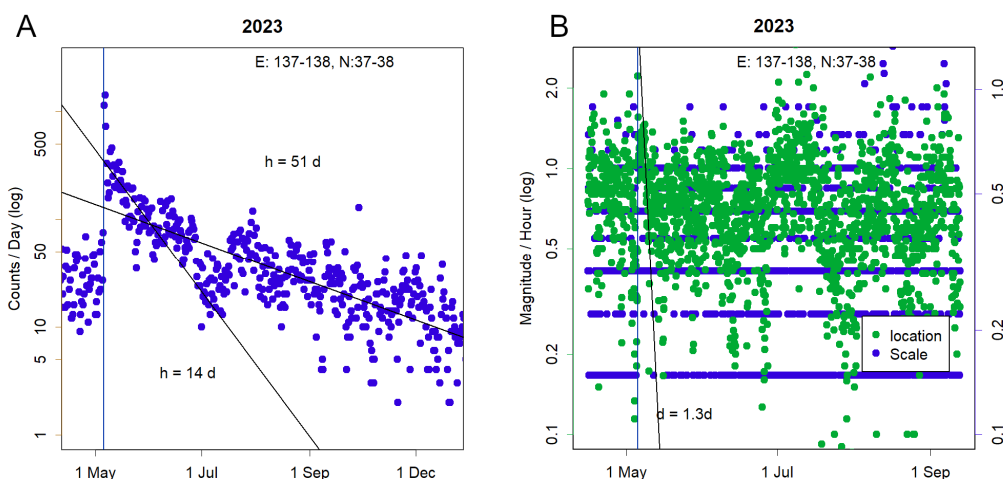


**Figure 2.** **A.** Number of aftershocks observed in 12 hour intervals. The semi logarithmic plot exhibits an approximately linear decay, consistent with previously reported half life behaviour [2]. **B.** Hourly estimates of the magnitude parameters. The locator shows only a brief and very small increase immediately after the 5 May event, returning to baseline within a short period. In contrast, the increase observed from September onward is more pronounced and persistent.

A rare sequence of earthquakes similar to the Noto case occurred recently in a different region. These events took place near the northernmost end of the Sanriku boundary, slightly offset toward the subducting Pacific Plate rather than directly on the boundary itself (Figure S1). Two earthquakes occurred in adjacent areas on 9 November 2025 (M6.9) and 8 December 2025 (M7.5). This region has long been characterised by elevated locator values, yet because it lies offshore, the available data are sparse and often overlooked. As a result, these earthquakes occurred without any clearly identifiable anomalies beforehand.

Although the aftershocks of these events decayed with a half-life (Figure S1C–D), the increase and subsequent decay in magnitude parameters were not particularly pronounced (Figure S1E–F). When averaged over longer time intervals, these changes become almost undetectable. Given the extremely short half-life, the estimated values are not especially precise. It is possible that the hypocentres have not yet fully released the accumulated energy. In this sense, the sequence may represent a precursor swarm preceding a larger mainshock. Because the events already reached substantial magnitudes, any subsequent mainshock could potentially be very large.

As shown in Figure S1B, the nationwide mesh used for the 2026 assessment is shifted by  $0.5^\circ$ , while maintaining a grid size of  $1^\circ$ . This adjustment was made because the original mesh boundaries would otherwise intersect four tiles, complicating the analysis. The  $1^\circ$  tile size remains consistent throughout, as it provides a practical resolution for analyzing seismic activity in Japan. For further details, see also Figure 3. Figure 3A shows a regional map of the study area based on the Ministry of Land, Infrastructure, Transport and Tourism dataset [3]. The map spans a 2 degree grid in both latitude and longitude, matching the scale used in Figures 3 and 4. The peninsula shown is Noto, and the island in the upper right is Sado Island, separated from Honshu. Figure B–F show annual distributions of earthquake epicentres. Green symbols indicate events with magnitudes  $M > 4$ . An increase in seismicity is evident near the eastern tip of the Noto Peninsula beginning around 2020. The year 2023 shows a particularly high number of events due to the M6.5 earthquake on 5 May and its subsequent aftershocks.

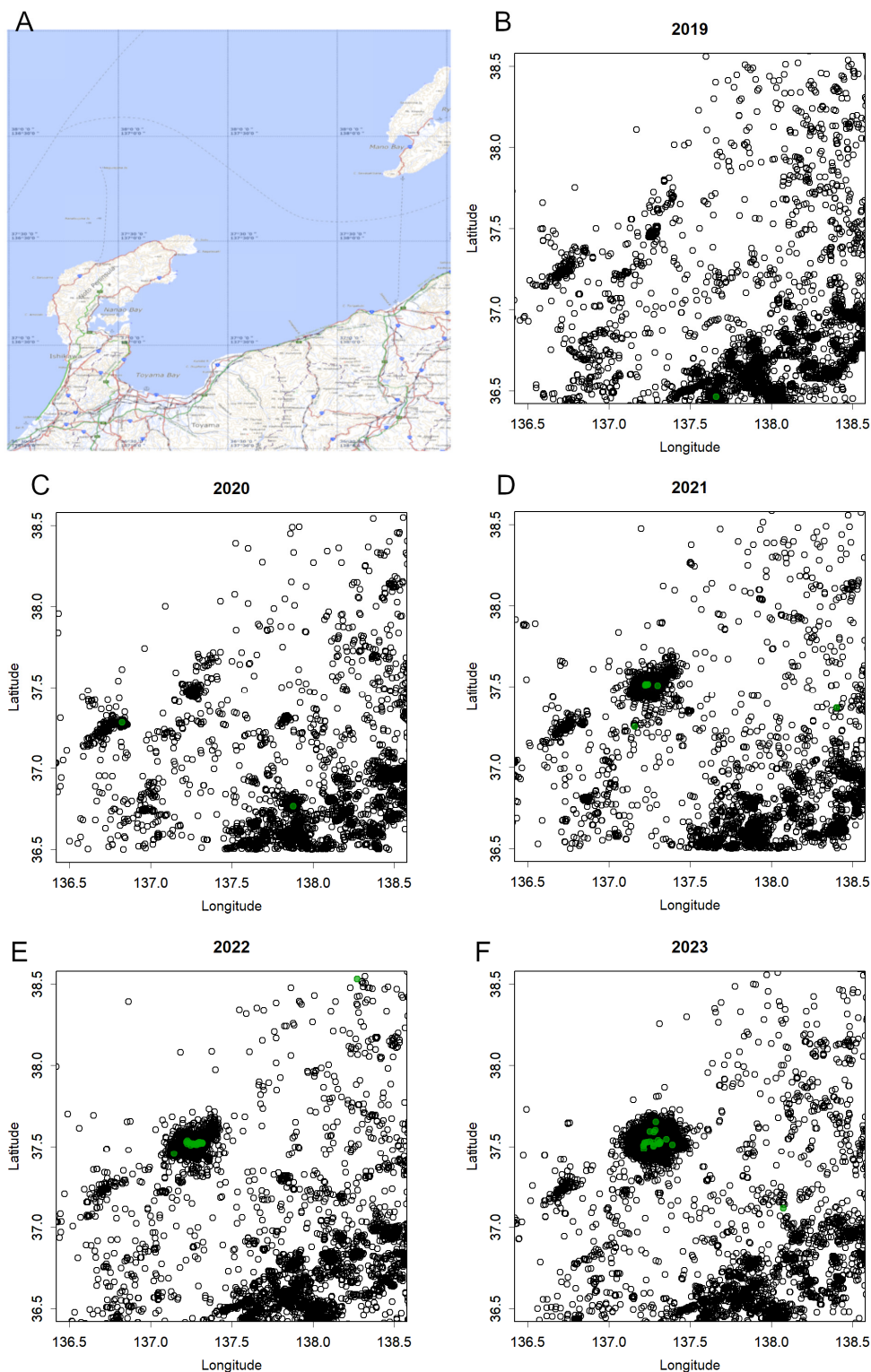


**Figure 3.** A. Standard map from the Ministry of Land, Infrastructure, Transport and Tourism [12]. Although shown at the same scale as the subsequent panels, it covers a slightly wider area due to its larger original size. The regions depicted in panels B–F are positioned almost entirely within this map. B–F. Annual distributions of earthquake epicentres. Green symbols denote events with magnitudes  $M > 4$ . A progressive increase in seismicity is evident near the tip of the Noto Peninsula. In panel F (2023), the elevated number of epicentres reflects the M6.5 earthquake on 5 May and its subsequent aftershocks.

Following the earthquake on 1 January 2024, the spatial pattern of seismicity changed markedly. Epicentres expanded from the entire Noto Peninsula westward into the offshore region (Figure 4A).

The triggering M7.6 earthquake occurred at the tip of the peninsula at 16:10, but within an hour, seismic activity had already propagated westward into the ocean. Notably, this offshore area corresponds to the epicentral region of the M6.9 earthquake that occurred on 25 March 2007 (Figure 4B).

Both in 2007 and throughout the period up to 2023, earthquakes in this region have been shallow, typically occurring at depths of around 20 km and at most reaching the depth of the Mohorovičić discontinuity (Figure 4C–D). The deeper seismicity corresponds to the Sanriku boundary. The relationship between this boundary and the earthquakes in 2023 and 2024 remains unclear. No large earthquakes have been recorded along the boundary itself, and the number of events does not appear to have increased significantly. These earthquakes are therefore interpreted as originating within the shallow seismic zone [3], reflecting stress accumulation associated with the horizontal thrusting of the Pacific Plate.

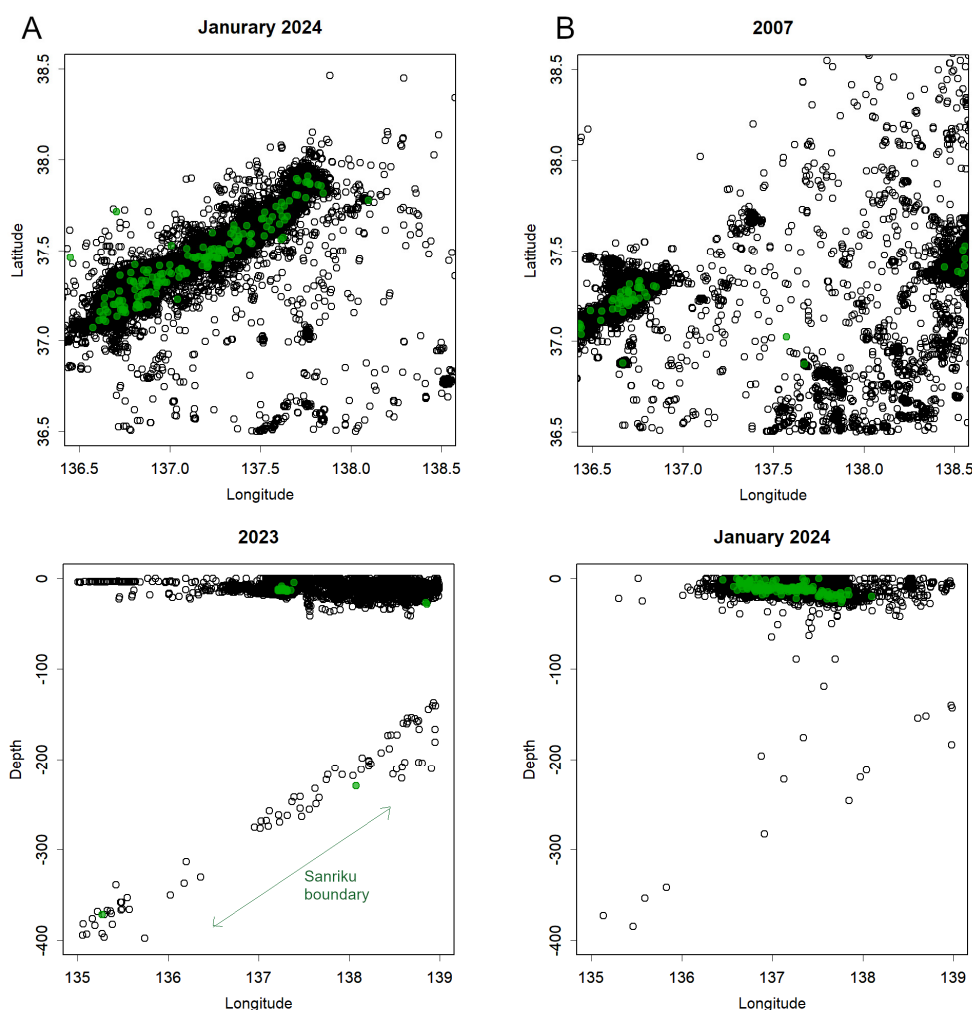


**Figure 4.** A. Immediately after the M7.6 earthquake on 1 January 2024, seismic activity expanded into the offshore region west of the Noto Peninsula, forming the pattern shown in panel A within one month. B. This offshore area corresponds to the epicentral region of the 25 March 2007 M6.9 earthquake. C–D. Epicenters. They are fundamentally shallow, typically occurring above ~20 km depth. Events deeper than 200 km are limited to those located along the Sanriku boundary. Along the boundary itself, neither the number of earthquakes nor the occurrence of large events has increased.

A characteristic feature of the offshore region west of the Noto Peninsula is the frequent occurrence of relatively high locator values. Although this tendency is more pronounced on the Pacific side, where the onshore portion of the plate boundary lies, this particular area on the Sea of

Japan side stands out for exhibiting exceptionally high locator values and elevated event frequency (Figure 5A–C). In contrast, the scale in this region is often very low (Figure 5D). Figure 5D corresponds to the same data shown in Figure 1B but with inverted colouring to highlight areas of low scale.

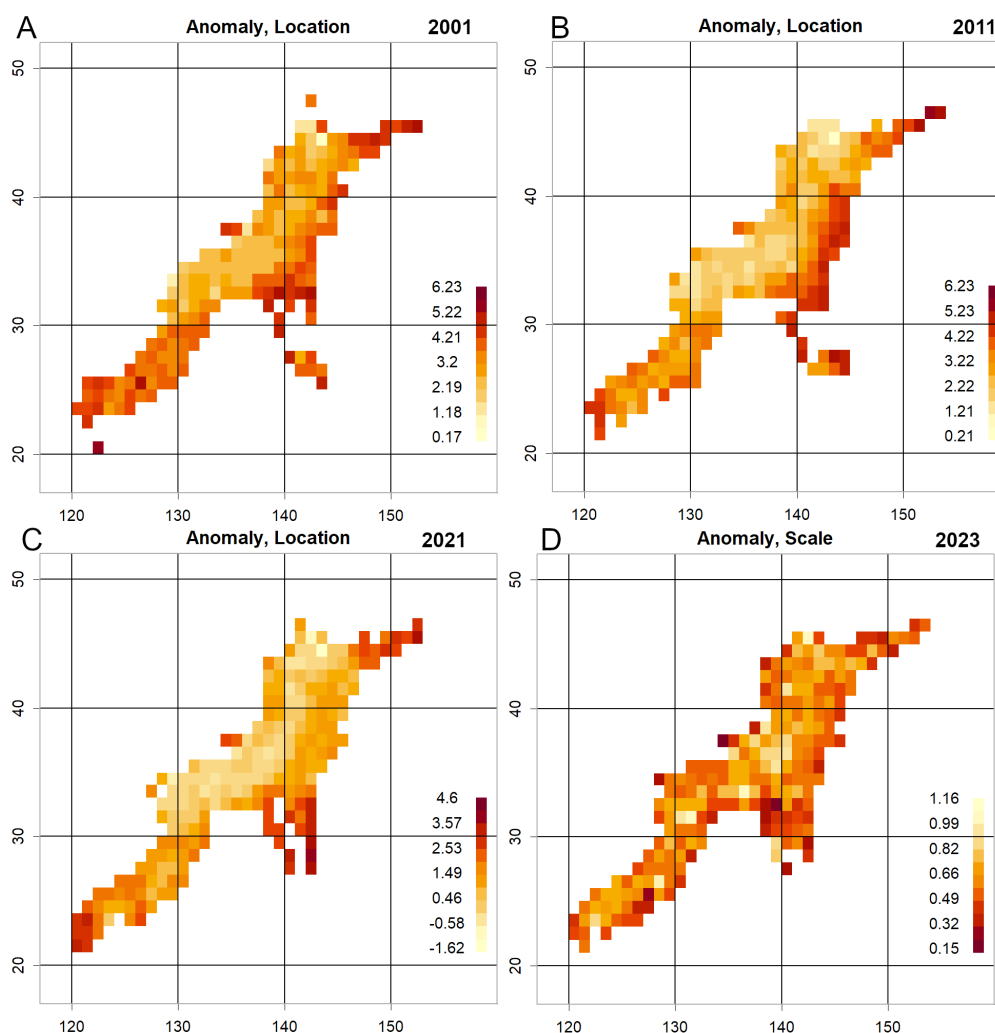


**Figure 5.** A–C. The offshore region west of the Noto Peninsula frequently exhibits elevated magnitude locator values, a tendency more pronounced here than in other areas on the Sea of Japan side [3]. D. In 2023, the scale in this region became extremely low. This panel shows the same data as Figure 1B but with inverted colouring to highlight low scale areas. A combination of high earthquake frequency and low scale is characteristic of seismic patterns observed in volcanic regions during periods of heightened volcanic activity [3]. The Noto Peninsula is located approximately between 136.7°E–137.3°E and 36.8°N–37.5°N. The elevated locator values in this area correspond to the two adjacent grid panels spanning 134°–136°E and 37°–38°N. These panels also coincide with the region where the scale decreases, as shown in Figure 5D. Together, they represent the shallow offshore area northwest of the Noto Peninsula.

The combination of high earthquake frequency and low scale resembles the precursory patterns observed prior to volcanic activity in the Tokara Islands, Miyakejima, and Mount Aso [3]. These regions commonly exhibit swarms of small earthquakes when magma or hydrothermal fluids begin to migrate. Such processes generate frequent low-magnitude events, and in some cases, larger earthquakes can occur without clear warnings [3].

Bathymetric data indicate that the seafloor in the offshore area adjacent to the Noto Peninsula is only about 100 metres deep, suggesting the possible presence of a submarine volcanic structure or a similar geological feature. Although direct evidence is limited, the seismic characteristics in this

region are consistent with those typically associated with volcanic-type activity, such as a bank of fine silt and low Bouguer anomalies [13]. These are examples of geological survey reports that describe sediment types and the presence or absence of gravity anomalies. Determining whether a volcanic structure is actually present would require a more detailed investigation of the seafloor, potentially using additional measurement techniques. However, such data are not currently available in the public domain, and thus could not be incorporated into this study. It is therefore plausible that the 1 January 2024 earthquake occurred when unreleased tectonic stress at the tip of the Noto Peninsula was triggered at a time when the surrounding offshore region was experiencing an elevated level of volcanic-type seismicity. The coincidence of these two conditions may have contributed to the generation of a large and damaging earthquake.

In this sense, the combination of a high locator in Figure 1C and a low scale in Figure 5D should have been noted as a potentially important signal. Although unconfirmed, the Noto region may also harbour volcanic hazards. It should be noted, however, that the reverse relationship does not always hold: some volcanic regions, such as Sakurajima, exhibit active volcanism without a corresponding decrease in scale.

Shallow seismic zones form discontinuous bands, a pattern that becomes particularly clear when analysis is restricted to very shallow hypocentres. Figure 6 displays earthquakes shallower than 5 km, thereby emphasising primarily volcanic type events (for example, Cape Erimo in the Kurils; Mount Akita Komagatake; the Hida Mountains including Mount Norikura and Mount Ontake; Miyakejima; Mount Aso; and the Tokara Islands). The offshore sources shown in Figure S1 are also visible because they occurred during the same interval. A band immediately south of these features follows the Pacific coastline. These shallow seismic zones lie closer to the Pacific Plate side than the surface tangent to the Sanriku boundary, suggesting that similar structures can form on the advancing plate as well.

At plate boundaries, contact and friction generate earthquake energy when frictional resistance is overcome. By contrast, shallow seismic zones appear to be regions where plate pressure is not readily released; instead, energy accumulates through crustal deformation. Several such shallow bands run roughly parallel to the line where crustal blocks overlap across the boundary.

Also apparent is a line extending from the Noto Peninsula to Sado Island. This feature may represent a distinct, unusually shallow segment among the shallow seismic zones and could accommodate Pacific Plate thrusting more readily than adjacent zones. The cause of this behaviour is unclear; one possibility is that it marks a marginal segment of the Eurasian Plate analogous to the Amur Plate [14,15]. A long, active fault is known along the northern coast of the Noto Peninsula [13], and seismic activity in the region has been associated with uplift of the peninsula [16,17]. Such plate driven orogenic processes contribute to the formation of the Japanese archipelago. Alternatively, continued uplift could eventually extend Noto eastward toward Sado Island. Historical precedent exists: an 1804 earthquake on the same Sea of Japan coast produced a 25 km wide uplifted strip at Kisakata that remains a notable landscape feature today [18].

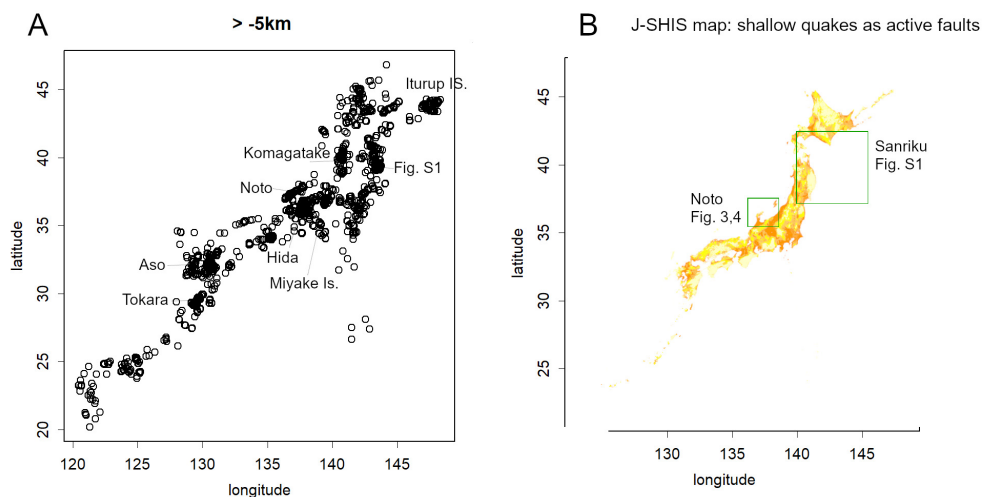


**Figure 6. A.** Epicentres shallower than 5 km (data from October 2025 to January 2026). Shallow events are concentrated where volcanic activity has been reported; the offshore clusters shown in Figure S1 are also visible because they occurred during the same interval. A shallow band immediately south of these features follows the Pacific coastline and corresponds to the shallow seismicity highlighted in Figure S1. The line extending from the Noto Peninsula to Sado Island lies on the Eurasian Plate and is subject to compressive loading; under the present filtering this segment appears unusually dominated by very shallow earthquakes. **B.** J-SIS Japan Seismic Hazard Information: shallow earthquakes and active faults [19], shown at the same scale as panel A. Inset (green outlines). Left outline: area shown in Figure 3; right outline: approximate extent of Figure S1.

In the 2024 event, the locator rose prior to declining with a characteristic half life (Figure 7A), a behaviour commonly observed following mainshocks [3], suggesting substantial energy release. The subsequent aftershock sequence, however, displays an unusual trajectory. After an initial decay consistent with a half life, the rate of aftershocks ceased declining after roughly two weeks and, unexpectedly, began to increase again. The cause of this resurgence is unknown, and no contemporaneous large earthquake has been identified to account for it. As of 2026, magnitudes remain relatively low (Figure 7C), and although aftershocks continue, their activity appears to have partially stabilized (Figure 7D). No clear small scale or high/low locator patterns have been detected (Figure 7E–F). Nevertheless, the region remains susceptible to major earthquakes and may be undergoing ongoing orogenic processes; continued vigilant monitoring is therefore warranted.

While the Noto sequence exhibited persistent elevation in locator values and complex aftershock dynamics (Figure 7A), similar behavior was not observed in recent events near the Sanriku boundary (Figure S1). This contrast suggests that the nonstationary features identified in Noto may not be universally applicable across all tectonic settings in Japan. The absence of comparable precursory signals in Sanriku underscores the importance of tailoring seismic monitoring approaches to the specific characteristics of each region.

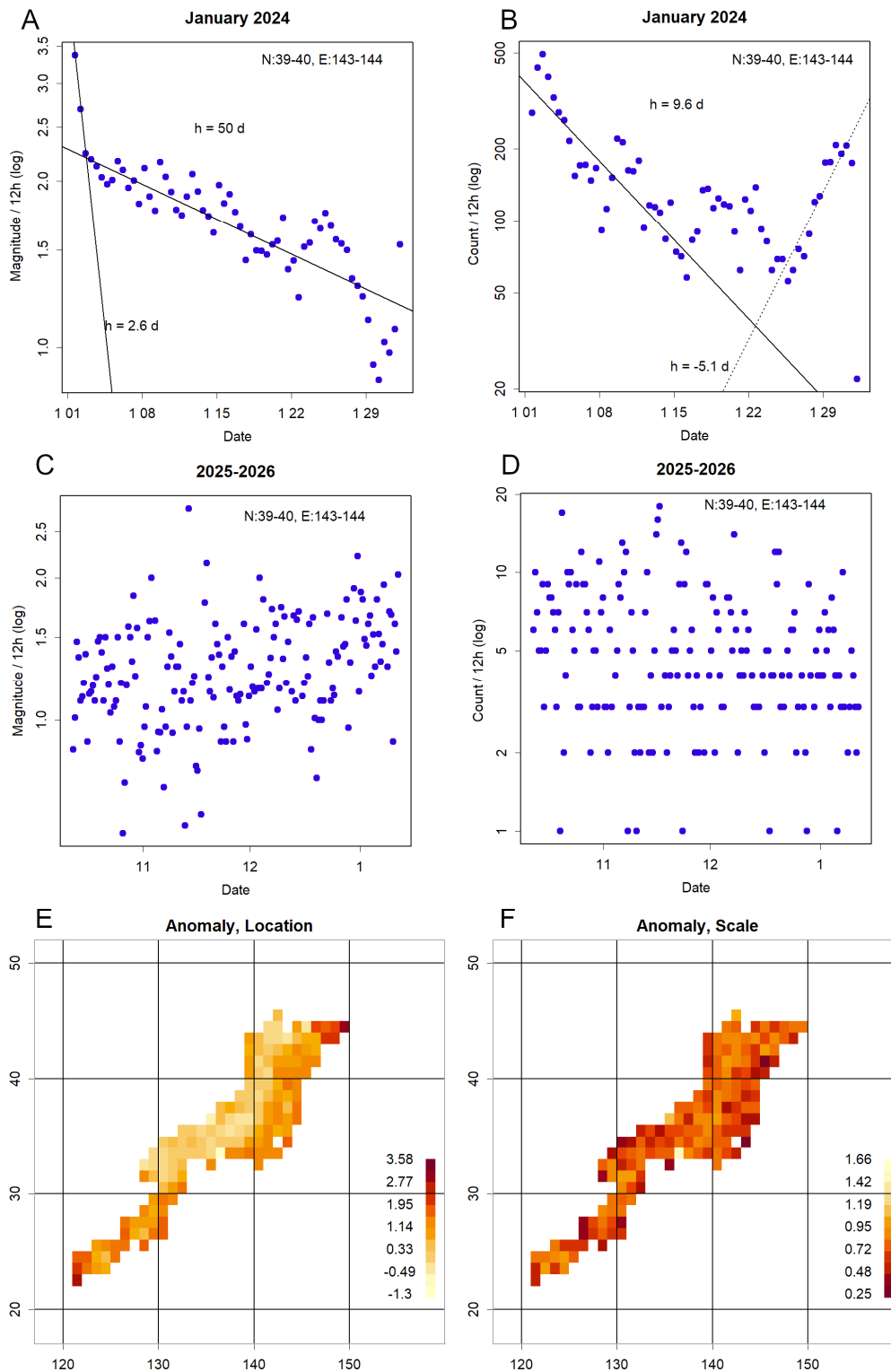


**Figure 7.** A. Twelve hour average magnitude during the M7.6 earthquake on 1 January 2024. Magnitudes are clearly elevated during the mainshock and then decline approximately linearly, a trend more pronounced than that shown in Figure 2B. B. Aftershock counts (12 hour intervals). After an initial linear decrease, the aftershock rate ceased declining after roughly three weeks and subsequently increased—an unusual pattern that contrasts with the behaviour in Figure 1A. C–D. Twelve hour average magnitude and aftershock data for October 2025 to January 2026. Both metrics remain at low levels during this interval. E–F. Mesh derived locator and scale data for 2025–2026. Locator values near Noto are not elevated, and no decrease in scale is observed. No significant anomalies have been observed around the Noto Peninsula.

## 4. Conclusion

Although advanced visualization methods for seismicity have been developed, effective use of these tools requires experience. Regional variability in seismic behaviour is evident, and there are geodynamic reasons why some areas are more earthquake prone than others. In this study we examined the frequent seismicity of the Noto Peninsula and assessed potential avenues for short term indication. The offshore region west of Noto may host previously undetected submarine volcanic or volcano related structures; this possibility, together with evidence for ongoing orogenic deformation, argues for continued, ideally annual, monitoring of epicentral activity. Moreover, following any large event it is essential to verify whether accumulated energy has been sufficiently released. In this respect, the recent sequence off the Sanriku coast merits sustained attention.

**Supplementary Materials: Supplementary Materials:** The following supporting information can be downloaded at the website of this paper posted on Preprints.org. Figure S1: Two recent earthquakes at Sanriku boundary.

**Funding:** This research received no external funding.

**Data Availability Statement:** All the data used can be downloaded from JMA homepage [7, 8]. R source code is available in Zendo <https://doi.org/10.5281/zenodo.17983155>.

**Conflicts of Interest:** The authors declare no conflicts of interest.

## Abbreviations

The following abbreviations are used in this manuscript:

JMA      Japan Meteorological Agency

## Appendix A Distribution of Magnitude and the GR Law

Histograms are often used for a simple examination of data distribution. However, for a more rigorous check, modern statistical methods such as EDA provide the Q-Q plot method. This involves comparing the quantiles of the data (data points at a given percentage position when sorted in descending order) with the corresponding quantiles of an ideal distribution. Ideally, one should prepare an ideal distribution with the same number of data points and compare the sorted data with this ideal distribution. If the data follows that distribution pattern, the comparison will form a straight line (Figure 11A). Indeed, when sorting the magnitude data aggregated monthly and comparing it with an ideal normal distribution, a straight line is obtained (Figure 11B). In this case, no data points are ignored. Magnitudes do follow a normal distribution.

Now, when we plot the histogram of normally distributed random numbers, we obtain the familiar bell-shaped graph (Figure 11C). However, when plotted on a semi-log graph, it takes on a cannonball shape instead (Figure 11D). At this point, the right-hand end appears to show a linear relationship. In reality, this is a pseudo-relationship; the larger the data, the steeper the slope becomes. And this is merely a graphical artefact, having no mathematical significance. It probably has no physical meaning either.

Given these properties, if we apply the GR law to the normally distributed data of B, we will also get a straight line. However, this would necessitate filtering out and disregarding most data points with weaker magnitudes. In rigorous science, selecting data to suit the analyst's convenience is termed cherry-picking and is regarded as data manipulation, which is to be criticized and avoided.

It is important to note that applying a logarithmic transformation to a dataset that is already approximately normally distributed is not a statistically sound practice. Such a procedure can distort the underlying distribution and obscure meaningful patterns. The conventional estimation of the b-value, which relies on this transformation, may therefore suffer from reduced precision and interpretability in such contexts. Moreover, the b-value is not directly related to the location ( $\mu$ ) or

scale ( $\sigma$ ) of the original magnitude distribution, and thus captures a different aspect of seismicity. In contrast, the locator and scale parameters provide a direct and intuitive characterization of the central tendency and dispersion of magnitudes, respectively, without requiring transformation.

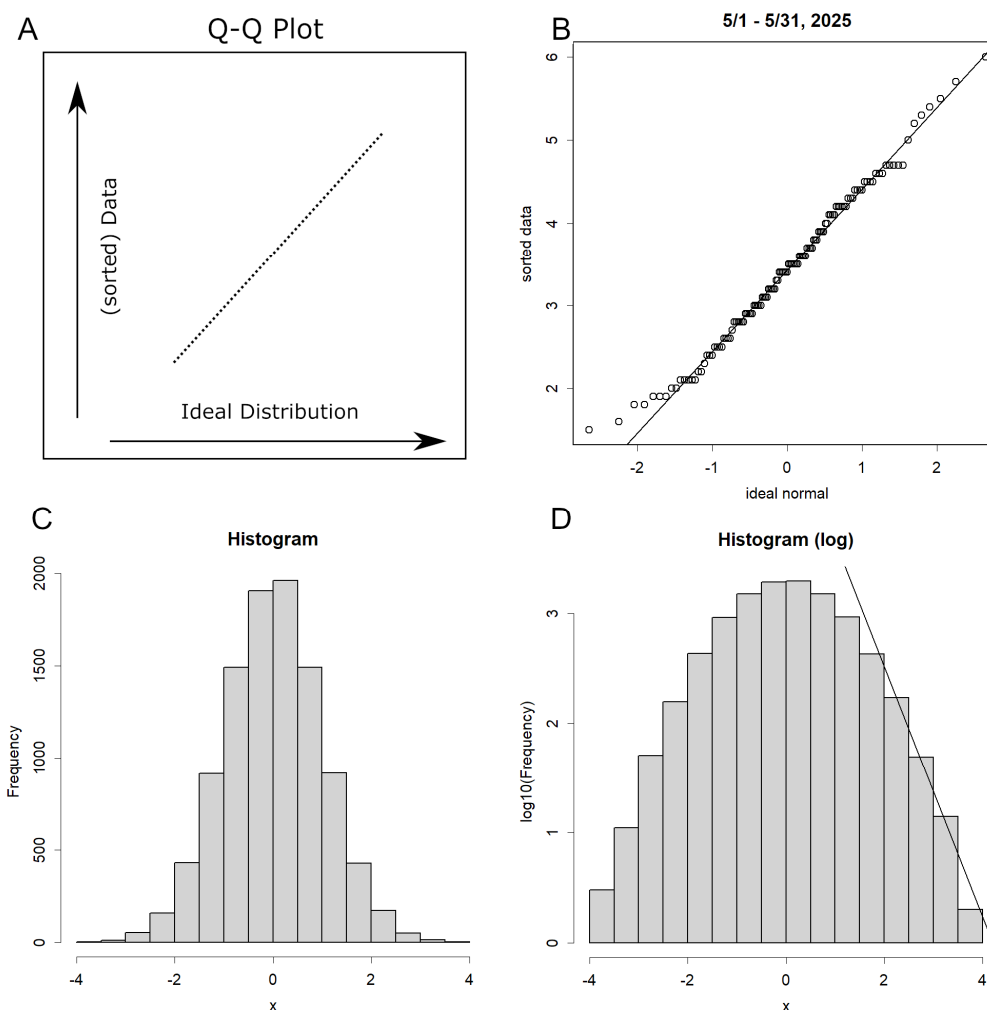


**Figure 8.** The concept of a Q-Q plot. It compares quantiles of data on the y-axis and an ideal distribution on the x-axis. If the data follows the distribution, the relationship will be a straight line. B. Example of a normal Q-Q plot using data from March 2025. The x-axis shows an ideal normal distribution. Data were obtained from the Japan Meteorological Agency (JMA) [6], which compiled the magnitude of all perceptible earthquakes. C. Histogram of normally distributed random numbers. D. The same histogram plotted on a semi-logarithmic scale. A straight line is fitted to the rightmost portion of the distribution, representing the slope corresponding to the  $b$ -value in the Gutenberg–Richter (GR) law. However, since the underlying distribution cannot be linear in principle, this estimation entails substantial error. Above all, this relationship applies only to the relatively large magnitudes at the far right, meaning the bulk of the data, including the median, is ignored.

## References

1. JMA. How Earthquakes Occur Available online: [https://www.data.jma.go.jp/svd/eqev/data/jishin/about\\_eq.html](https://www.data.jma.go.jp/svd/eqev/data/jishin/about_eq.html) (accessed on 28 January 2026).
2. JMA. About earthquake prediction. Available online: <https://www.jma.go.jp/jma/kishou/known/faq/faq24.html> (accessed on 28 January 2026).
3. Konishi, T. Review: Exploratory Data Analysis with R: A New Approach to Seismic Data. *Preprints* 2025, doi:10.20944/preprints202512.1377.v2.
4. Tukey, J.W. *Exploratory data analysis*; Reading, Mass. Addison-Wesley Pub. Co.: London, 1977.

5. NIST/SEMATECH. e-Handbook of Statistical Methods. Available online: <http://www.itl.nist.gov/div898/handbook> (accessed on 28 January 2026).
6. JMA. Earthquake Monthly Report (Catalog Edition). Available online: <https://www.data.jma.go.jp/eqev/data/bulletin/hypo.html> (accessed on 28 January 2026).
7. R Core Team. R: A language and environment for statistical computing; R Foundation for Statistical Computing: Vienna, 2025.
8. JMA. Summary of seismic activity for each month. Available online: <https://www.data.jma.go.jp/eqev/data/gaikyo/> (accessed on 28 January 2026).
9. Thornton, S., (Ed.) Karl Popper. Metaphysics Research Lab, Stanford University: 2023.
10. Omori, F. On the After-shocks of Earthquakes. *The journal of the College of Science, Imperial University, Japan*. Available online: <https://repository.dl.itc.u-tokyo.ac.jp/records/37571> (accessed on 28 January 2026).
11. Utsu, T. Magnitude of earthquakes and occurrence of their aftershocks. *Journal of the Seismological Society of Japan*. 2nd ser. 1957, 10, 35-45, doi:10.4294/zisin1948.10.1\_35.
12. Geospatial Information Authority of Japan (GSI). Standard map. Available online: <https://maps.gsi.go.jp/> (accessed on
13. Geological Survey of Japan. Seamless geoinformation of coastal zone "Northern coastal zone of Noto Peninsula" Available online: <https://www.gsj.jp/researches/project/coastal-geology/results/s-1.html> (accessed on 28 January 2026).
14. Bird, P. An updated digital model of plate boundaries. *Geochemistry, Geophysics, Geosystems* 2003, 4, doi:<https://doi.org/10.1029/2001GC000252>.
15. Malyshev, Y.F.; Podgornyi, V.Y.; Shevchenko, B.F.; Romanovskii, N.P.; Kaplun, V.B.; Gornov, P.Y. Deep structure of the Amur lithospheric Plate border zone. *Russian Journal of Pacific Geology* 2007, 1, 107-119, doi:10.1134/S1819714007020017.
16. JMA. Related information on the 2024 Noto Peninsula Earthquake. Available online: [https://www.jma.go.jp/jma/menu/20240101\\_noto\\_jishin.html](https://www.jma.go.jp/jma/menu/20240101_noto_jishin.html) (accessed on 28 January 2026).
17. Fujiwara, K. Coastal uplift and topographic changes caused by the Noto Peninsula earthquake. Available online: <https://rebootsuzu.com/noto/20250303/> (accessed on 28 January 2026).
18. Hirano, S.; Nakata, T.; Imaizumi, T. Crustal Shin-ichi Deformation Earthquake Sea Coast, Associated of with the 1804 on the Japan Northeast Japan. *The Quaternary Research* 1979, 18, 17-30, doi:<https://doi.org/10.4116/jaqua.18.17>.
19. National Research Institute for Earth Science and Disaster Resilience. J-SHIS Japan Seismic Hazard Information. Available online: <https://www.j-shis.bosai.go.jp/map/?lang=en> (accessed on 28 January 2026).

**Disclaimer/Publisher's Note:** The statements, opinions and data contained in all publications are solely those of the individual author(s) and contributor(s) and not of MDPI and/or the editor(s). MDPI and/or the editor(s) disclaim responsibility for any injury to people or property resulting from any ideas, methods, instructions or products referred to in the content.